J. Fluid Mech. (1983), *vol.* 136, *pp.* 243–267
Printed in Great Britain

The dispersion of solute from time-dependent releases in parallel flow

By N. G. BARTON
CSIRO Division of Mathematics and Statistics, PO Box 218, Lindfield, N.S.W., Australia 2070

(Received 9 May 1983)

This paper examines an often overlooked point in the theory of dispersion of passive contaminants in parallel flows – the behaviour of a cloud of solute which has been injected into the flow over a period of time. The problem is linear if the solute has neutral buoyancy and the diffusivity is independent of concentration, and so it can be treated by a Fourier transform in time. For such a Fourier-transform method to be successful, a non-standard eigenvalue problem has to be solved to determine the concentration pattern, the speed at which it is convected downstream and its decay distance downstream. The eigenvalue problem is not self-adjoint, the eigenvalue enters it nonlinearly if longitudinal diffusion is included, and it involves both regular and singular perturbation aspects. The eigenvalue problem is examined generally and the conclusions of Chatwin (1973*a*) are re-assessed. The eigenvalue problem is then solved numerically for three cases of interest. Two of these cases (dispersion from a harmonically varying source in Poiseuille and plane Couette flow) reveal most unusual eigenvalue structure, whilst the third (dispersion from a harmonically varying source in turbulent channel flow) is not exceptional. The effect of weak longitudinal diffusion is examined theoretically (for general applications) and numerically in one instance (the application to Poiseuille flow). Longitudinal diffusion, even if weak, has a marked effect on the eigenvalue structure. The paper concludes with a suggestion for an alternative attack on the original problem of dispersion from time-dependent sources.

1. Introduction

This paper considers the dispersion of a cloud of soluble matter which has been injected over a period of time into a steady parallel flow. This physical problem occurs in all dispersion experiments in parallel flows since it is experimentally impossible to inject solute into a flow in other than a time-varying manner. Of course, at extremes, the injection of solute may be accomplished in very short intervals in an attempt to inject a δ-function, or the injection may be maintained at a steady or almost steady rate. Inevitably, however, time-dependent injection will occur in experiments.

The theory underlying the time-dependent injection problem has a relatively short history, being primarily developed from Taylor's (1953) work on the dispersion of a finite cloud of solute. The problem was brought to the author's attention by chemists who were interested in using a gas-flow reactor (Howard 1976) to measure diffusion coefficients between gaseous species at low pressures. In their experiments (Plumb, Ryan & Barton 1983), the injection of the contaminant gas (oxygen) into the carrier gas (helium) flowing at about 10 m s^{-1} took place in about 20 ms, and the time-dependent injection effects had a pronounced effect on the oxygen distribution

measured further down the reactor. Some other particular applications for the theory have been reported by Brinkman (1950, viscosity-measuring experiments), Carrier (1956, an inverse problem in concentration measurement), Philip (1963*a*, *b*, micrometeorology and possibly physiology and botany) and Soundalgekar & Gupta (1977, magnetohydrodynamics). The most important unifying reference on the subject is due to Chatwin (1973*a*), who investigated dispersion from harmonically time-dependent inputs. Chatwin consolidated the previous references, gave a more general description of the problem, obtained high- and low-frequency approximations for two simple parallel flows, and developed methods for determining the most important features – the speed at which the concentration pattern is transported downstream and its decay distance in the downstream direction.

In general, dispersion from a time-dependent input can be investigated in two ways: the first is by recognizing the problem to be linear and proceeding through a Fourier transform in time. This was the method used by Chatwin, and it leads to an unusual eigenvalue problem which proves to be richer in detail than his asymptotic expansions would suggest. The second method is by regarding the input strength as a distribution of δ-functions in time, and therefore convolving the input distribution function with the solutions for dispersion from a δ-function input. This approach is becoming more attractive as the problem of dispersion from a δ-function input becomes better understood (Gill & Sankarasubramanian 1970; Chatwin 1970; Smith 1981).

The present paper is mainly concerned with exploring the viability of the first approach. In §2 the problem is specified mathematically, and the unusual eigenvalue problem mentioned above is obtained. Chatwin's (1973*a*) results (based on Fourier decomposition in time) are summarized and particular and interesting features of the eigenvalue problem are identified for subsequent investigation. One of these features is that the eigenvalue enters nonlinearly into the eigenvalue problem if longitudinal diffusion effects are included. The numerical methods required for the subsequent investigation are also described in §2. Then, in §§3, 4 and 5, numerical details are presented for dispersion from time-dependent sources in three basic flows in which longitudinal diffusion is neglected. High- and low-frequency asymptotic solutions were obtained for the first two problems (Poiseuille and plane Couette flow) by Chatwin (1973*a*), and the third set of results (for a model of turbulent channel flow) is believed to be new. The first two problems are found to have very unusual features associated with near-coalescence of eigenvalue branches. In §§6 and 7 effects of longitudinal diffusion are included and the eigenvalue problem in which λ enters nonlinearly is studied. Weak longitudinal-diffusion effects are calculated theoretically for general basic flows, and detailed numerical results are then presented for Poiseuille flow. A final discussion section concludes the paper. To highlight the most important conclusions: the problem is amenable to two methods of attack and the smeared out δ-function approach is recommended if asymptotic results at large time are required; unusual results are found numerically for Poiseuille and plane Couette flow even when longitudinal diffusion is neglected; and weak longitudinal diffusion changes the eigenvalues markedly.

2. Representation of the solution, some general results and numerical techniques

In this section the problem is mathematically specified, some results of Chatwin (1973*a*) are reviewed and extended, and the numerical techniques required for

subsequent applications are described. Suppose that a solute is injected over a period of time into the steady parallel flow $(UV(Y,Z),0,0)$ through a cross-section with typical dimension a. Here U is the discharge speed of the flow, and the problem is specified in dimensional Cartesian coordinates (x, aY, aZ), where x is a distance in the direction of the flow. Throughout the presentation, an overbar will denote the cross-sectional mean, so that $\overline{V} = 1$ by construction. It will be assumed that the diffusion coefficient of the solute in the solvent can be written $DK(Y,Z)$, where D is dimensional and $\overline{K} = 1$. The dependence of K on Y, Z allows for idealized problems where the diffusive fluxes are isotropic yet possibly varying in strength across the cross-section. Moreover the fluxes are independent of the concentration C of solute. If the injected solute is neutrally buoyant and if ∇ denotes the operator $(0, \partial/\partial Y, \partial/\partial Z)$, the concentration C of solute is specified by the problem

$$\frac{\partial C}{\partial t} + UV(Y,Z)\frac{\partial C}{\partial x} = DK(Y,Z)\frac{\partial^2 C}{\partial x^2} + \frac{D}{a^2}\nabla\cdot(K(Y,Z)\nabla C), \tag{2.1a}$$

$$K\frac{\partial C}{\partial n} = 0 \quad \text{at the boundary.} \tag{2.1b}$$

For this linear problem, the concentration at the injection point $x = 0$ (say) can be represented by superposition of spectral components. Without loss of generality, therefore, the condition at $x = 0$ is taken to be

$$C(0, Y, Z, t) = g(Y,Z)\,\mathrm{e}^{\mathrm{i}\omega t}, \tag{2.1c}$$

with $0 \leqslant \omega < \infty$. The problem $(2.1a, b)$ has separable solutions

$$C = \exp\left\{\mathrm{i}\omega\left(t - \frac{\lambda x}{U}\right)\right\}\psi(Y,Z,\Omega,\epsilon), \tag{2.2}$$

in which λ and ψ are the eigenvalue and eigenfunction in the eigenvalue problem

$$\nabla\cdot\{K(Y,Z)\nabla\psi\} = \mathrm{i}\Omega\{1 - \lambda V(Y,Z) - \mathrm{i}\epsilon\lambda^2 K(Y,Z)\}\psi, \tag{2.3a}$$

$$K\frac{\partial\psi}{\partial n} = 0 \quad \text{at the boundary.} \tag{2.3b}$$

Here the dimensionless parameters Ω and ϵ are defined by

$$\Omega = \frac{\omega a^2}{D}, \quad \epsilon = \Omega\left(\frac{D}{Ua}\right)^2; \tag{2.4}$$

thus Ω is a frequency parameter and ϵ is a measure of the importance of longitudinal diffusion. In many applications involving dispersion of matter in liquids, Chatwin (1973*a*) points out that ϵ is so small that longitudinal diffusion can be neglected. (For example, a typical value for κ for the diffusion of matter in liquids is $\kappa = 10^{-9}$ m^2 s^{-1}. If the values $\omega = 2\pi$ s^{-1} and $U = 10^{-2}$ m s^{-1} are chosen as representative of laboratory experiments, ϵ is then found to be $\epsilon = 10^{-6}$. The effects of longitudinal diffusion can therefore be neglected in (2.3*a*) provided λ is found to be $O(1)$, which is, in fact, confirmed by subsequent computations.) In contrast, if the dispersion of gas species at low pressures is considered as by Plumb *et al.* (1983), then ϵ is not small and longitudinal diffusion is important. (Typical values for the constants in the work of Plumb *et al.* were $a = 10^{-2}$ m, $\kappa = 0.02$ m^2 s^{-1}, $U = 10$ m s^{-1} and $\omega = 2\pi/0.01$ s^{-1}. These typical values for the constants give $\Omega = 3$ and $\epsilon = 0.1$; whilst other extreme values for the constants gave ϵ values greater than 1. Clearly, longitudinal-diffusion effects cannot be neglected in such applications.)

The eigenvalue problem (2.3) is non-standard because it involves complex-valued coefficients and because the eigenvalue λ enters quadratically if ϵ is not zero. (The eigenvalue already enters linearly into the problem by virtue of the second term on the right-hand side of (2.3*a*).) The occurrence of complex coefficients means that problem (2.3) is not self-adjoint, even when $\epsilon = 0$, and so the usual eigenvalue theory (e.g. Boyce & Di Prima 1977) is no longer applicable. Thus, whilst (2.3) may possess eigenvalues, these would almost inevitably be complex-valued; moreover it is possible that the corresponding set of eigenfunctions is not complete, that multiple eigenvalues exist, and that ordering and asymptotic properties of the eigenvalues would not be guaranteed as in self-adjoint systems. The non-self-adjointness of the problem is even more pronounced when $\epsilon \neq 0$, and it appears that few theoretical results have been established for problems as general and as complicated as (2.3). Two references should be noted in this context, however: Swanson (1978) has presented comparison theorems for problems such as (2.3), and Andrews (1974) has compiled a list of 300 references to problems in which the eigenvalue enters nonlinearly.

In the sequel, it will be *assumed* that V and K in (2.3) are such that the problem possesses a discrete set of (complex) eigenvalues $\{\lambda_p\}$ with corresponding eigenfunctions $\{\psi_p\}$. This allows some of Chatwin's conclusions to be re-examined when longitudinal diffusion is retained, i.e. $\epsilon \neq 0$. The first of these concerns orthogonality: standard manipulations on (2.3) give the result

$$0 = (\lambda_p - \lambda_q)\left\{\int\int V f_p f_q \,\mathrm{d}S - \mathrm{i}\epsilon(\lambda_p + \lambda_q)\int\int f_p f_q \,\mathrm{d}S\right\}, \tag{2.5}$$

where the integration is over the cross-section of the flow. This result shows that orthogonality of the eigenfunctions is lost when $\epsilon \neq 0$. If C is written as the superposition

$$C = \sum_p A_p(\Omega, \epsilon) \exp\left\{\mathrm{i}\omega\left(t - \frac{\lambda_p x}{U}\right)\right\} \psi_p(Y, Z, \Omega, \epsilon), \tag{2.6}$$

then the constants A_p are determined by fitting the injection condition (2.1*c*), so that $\Sigma_p A_p(\Omega, \epsilon)\,\psi_p(Y, Z, \Omega, \epsilon) = g(Y, Z)$. For this purpose, it is necessary to assume that the set of eigenfunctions $\{\psi_p\}$ is complete with respect to $g(Y, Z)$. The constants A_p are then determined by truncating and solving the infinite set of simultaneous equations

$$\sum_p A_p(\psi_p, \psi_q) = (g, \psi_q), \tag{2.7}$$

where the brackets denote an appropriate integral. This procedure is straightforward when the eigenfunctions are orthogonal, that is, when $\epsilon = 0$.

Chatwin (1973*a*) also deduced some elementary bounds for the eigenvalues and his treatment is now examined with $\epsilon \neq 0$. If complex conjugates are denoted by asterisks, (2.3*a*) gives for any particular eigenvalue

$$\nabla\cdot(K\nabla\psi) = \mathrm{i}\Omega(1 - \lambda V - \mathrm{i}\epsilon\lambda^2 K)\,\psi,$$

$$\nabla\cdot(K\nabla\psi^*) = -\mathrm{i}\Omega(1 - \lambda^* V + \mathrm{i}\epsilon\lambda^{*2} K)\,\psi^*,$$

and hence

$$\nabla\cdot(K\psi^*\nabla\psi) - K|\nabla\psi|^2 = \mathrm{i}\Omega(1 - \lambda V - \mathrm{i}\epsilon\lambda^2 K)\,|\psi|^2,$$

$$\nabla\cdot(K\psi\nabla\psi^*) - K|\nabla\psi|^2 = -\mathrm{i}\Omega(1 - \lambda^* V + \mathrm{i}\epsilon\lambda^{*2} K)\,|\psi|^2.$$

Integration of these equations over the cross-section and use of the boundary condition (2.3*b*) gives that

$$\lambda_I + \epsilon(\lambda_R^2 - \lambda_I^2)\frac{\int K|\psi|^2\,dS}{\int V|\psi|^2\,dS} = -\frac{1}{\Omega}\frac{\int K|\nabla\psi|^2\,dS}{\int V|\psi|^2\,dS}, \tag{2.8a}$$

$$\lambda_R - 2\epsilon\lambda_R\lambda_I\frac{\int K|\psi|^2\,dS}{\int V|\psi|^2\,dS} = \frac{\int |\psi|^2\,dS}{\int V|\psi|^2\,dS}. \tag{2.8b}$$

For $\epsilon = 0$ and $K,\ V \geqslant 0$, Chatwin deduced the bounds

$$\frac{1}{V_{\max}} \leqslant \lambda_R < \infty, \quad \lambda_I < 0, \tag{2.9}$$

but there is no simple extension of these results when ϵ is non-zero.

An ordering principle for the eigenvalues

It was implicitly assumed by Chatwin (1973*a*) that an ordering principle of the form

$$0 < -\operatorname{Im}(\lambda_0(\Omega, \epsilon)) < -\operatorname{Im}(\lambda_1(\Omega, \epsilon)) < \ldots$$

could be established for the eigenvalues, and that this ordering would hold for all values of Ω. (The fact that $\operatorname{Im}(\lambda_p) < 0$ ensures that all modes are spatially decaying.) One of the important results of the present work is that such an ordering principle may break down in some applications whether or not longitudinal diffusion is considered. However, in the applications investigated in §§3, 4, 5 and 7, the breakdown in ordering does not affect the dominant eigenmode characterized by λ_0. Thus the mode with the lowest absolute value of $\operatorname{Im}(\lambda(0,0))$ has the lowest absolute value of $\operatorname{Im}(\lambda)$ at all values of Ω, ϵ.

Dominant behaviour for large x and at high and low frequencies

For large x the series (2.6) has the leading term

$$C \approx A_0 \exp\left\{i\omega\left(t - \frac{\lambda_0 x}{U}\right)\right\}\psi_0(Y, Z), \tag{2.10}$$

where λ_0 is the eigenvalue defined by the ordering principle above. The concentration pattern is therefore convected at speed $U/\operatorname{Re}(\lambda_0)$ and decays in a longitudinal distance $-U/\omega\operatorname{Im}(\lambda_0)$. At high frequencies Chatwin showed that $\operatorname{Re}(\lambda_0)$ was expected to be near $1/V_{\max}$ with the concentration pattern confined to a region near where $V = V_{\max}$. For low frequencies, Chatwin deduced the result $\lambda_0(\Omega) = 1 - iA\Omega + O(\Omega^2)$, where A is a dimensionless number depending on the flow. In this case, the concentration pattern is convected at the discharge speed U and is approximately constant across the cross-section of the flow. Chatwin's arguments for high and low frequencies remain applicable even with longitudinal diffusion included ($\epsilon \neq 0$), although $\operatorname{Re}(\lambda_0)$ and $\operatorname{Im}(\lambda_0)$ change with ϵ. For instance, the effect of longitudinal diffusion on the constant A above is known for many applications by virtue of work by Aris (1956).

Numerical methods

Finite-difference methods and shooting methods were used to calculate the eigenvalues presented in subsequent sections. Brief descriptions of these two methods are given for the eigenvalue problem

$$-\frac{\mathrm{d}}{\mathrm{d}t}\left[p(t)\frac{\mathrm{d}u}{\mathrm{d}t}\right]+q(t)\,u=\{\lambda r(t)+\epsilon\lambda^2 s(t)\}\,u, \tag{2.11a}$$

$$\frac{\mathrm{d}u}{\mathrm{d}t}=0 \quad \text{at} \quad t=a,b, \tag{2.11b}$$

which is sufficiently general to cover all the examples subsequently considered. (Some mild conditions are needed on $p(t)$, $q(t)$, $r(t)$ and $s(t)$ for subsequent error estimates to be applicable.) For the finite-difference method, the differential problem (2.11) is discretized on a uniform mesh

$$t_0 < t_1 < t_2 < \ldots \quad \ldots \quad < t_{N-1} < t_N < t_{N+1}$$

with spacing $H=(b-a)/(N-1)$, where the points t_0 and t_{N+1} are fictitious points beyond the boundaries at $t_1=a$ and $t_N=b$. If the central-difference approximations

$$\frac{\mathrm{d}u}{\mathrm{d}t}=\frac{u_{j+1}-u_{j-1}}{2H}, \quad \frac{\mathrm{d}^2u}{\mathrm{d}t^2}=\frac{u_{j+1}-2u_j+u_{j-1}}{H^2}$$

are applied to (2.11a), the system of equations

$$u_{j-1}[-2p_j+Hp_j']+u_j[4p_j+2H^2\{q_j-\lambda r_j-\epsilon\lambda^2 s_j\}]+u_{j+1}[-2p_j-Hp_j']=0, \tag{2.12a}$$

is obtained for $j=1,\ldots,N$. The boundary conditions (2.11b) provide the extra conditions

$$u_0=u_2, \quad u_{N-1}=u_{N+1}, \tag{2.12b}$$

and these equations (2.12a,b) form a set of $N+2$ simultaneous homogeneous equations in $N+2$ unknowns. That is,

$$\boldsymbol{A}[u_0\,u_1\,\ldots\,u_{N+1}]^{\mathrm{T}}=\boldsymbol{0},$$

where the matrix $\boldsymbol{A}$ is tridiagonal, and the condition for (2.12) to have a solution is that $\det\boldsymbol{A}=0$. The discrete problem (2.12) yields N eigenvalues $\{\lambda_n^{(N)}\}_{n=1}^{N}$. For the case when $\epsilon=0$, the difference e_n between $\lambda_n^{(N)}$ and the nth eigenvalue λ_n of the differential problem (2.11) is known to satisfy (Paine & Anderssen 1980, equation (3.2))

$$|e_n|=|\lambda_n-\lambda_n^{(N)}|\leqslant CH^2\lambda_n^2. \tag{2.13}$$

(Here C is a constant independent of H and n, and this result does not apply for the case when $\epsilon\neq 0$ in (2.11, 2.12).) The eigenfunction corresponding to $\lambda_n^{(N)}$ may be determined by back-substitution after arbitrarily assigning a value to u at one of the endpoints.

For the shooting method, the problem (2.11) is replaced by the following system of first-order differential equations:

$$\frac{\mathrm{d}}{\mathrm{d}t}\begin{bmatrix}u\\v\end{bmatrix}=\begin{bmatrix}0 & 1/p\\ q(t)-\lambda r(t)-\epsilon\lambda^2 s(t) & 0\end{bmatrix}\begin{bmatrix}u\\v\end{bmatrix}, \tag{2.14a}$$

where

$$\begin{bmatrix}u\\v\end{bmatrix}=\begin{bmatrix}\text{arbitrary}\\ 0+\mathrm{i}0\end{bmatrix} \quad \text{at} \quad t=a. \tag{2.14b}$$

The value of $[u \quad v]^{\mathrm{T}}$ at $t = b$ was computed using the 4th-order Runge–Kutta technique, and the value of λ was adjusted until $v(b)$ was zero to within a prescribed tolerance. If the Runge–Kutta solution is achieved in N steps, then the error between the eigenvalues of the discrete and continuous problems satisfies (Paine & Anderssen 1980, equation (3.6))

$$|e_n| = |\lambda_n - \lambda_n^{(N)}| \leqslant CH^4\lambda_n^3, \quad C \text{ constant}. \tag{2.15}$$

(This result applies for the case $\epsilon = 0$.) The shooting method also gives an immediate numerical approximation to the corresponding eigenfunction.

Both numerical procedures were expedited using an efficient root-finding routine based on inverse quadratic interpolation. The computations were mainly performed on a PDP 11/34 minicomputer with selective checking on a CDC Cyber 76 computer. All the eigenvalues described in subsequent sections are considered to be accurate to 3 significant figures; and some detailed comparisons of the numerical methods are presented in table 2. Further checks on the numerical methods were made by comparisons with the asymptotic results of Chatwin (1973*a*) and with some exact solutions which applied in other special cases. The computation of the eigenfunctions also confirmed that the boundary condition (2.11*b*) was satisfied at $t = b$.

3. Results for Poiseuille flow, $\epsilon = 0$

The first example considered is the dispersion of a solute with constant molecular diffusivity κ injected as a function of time into laminar flow in a circular pipe of radius a. Here D becomes κ and $K = 1$, and, if R is defined by $R^2 = Y^2 + Z^2$, the velocity profile is $V(R) = 2(1-R^2)$. The eigenvalue problem (2.3) with longitudinal diffusion neglected ($\epsilon = 0$) becomes

$$\frac{1}{R}\frac{\mathrm{d}}{\mathrm{d}R}\left(R\frac{\mathrm{d}\psi}{\mathrm{d}R}\right) = \mathrm{i}\Omega[1-2\lambda(1-R^2)]\psi \tag{3.1a}$$

under the boundary conditions

$$\frac{\mathrm{d}\psi}{\mathrm{d}R} = 0 \quad \text{at} \quad R = 0 \quad \text{(by symmetry)} \quad \text{and} \quad R = 1. \tag{3.1b}$$

This problem has the solution (Philip 1963*a*)

$$\psi(R, \Omega) = \exp\{-\tfrac{1}{2}\beta R^2\} M(-\gamma, 1, \beta R^2), \tag{3.2a}$$

where

$$\beta = (2\mathrm{i}\lambda\Omega)^{\frac{1}{2}}, \quad \gamma = \left(\frac{\mathrm{i}\Omega}{2\lambda}\right)^{\frac{1}{2}}\left(\frac{2\lambda-1}{4}\right) - \tfrac{1}{2}, \tag{3.2b}$$

the square roots have positive real parts and M is Kummer's confluent hypergeometric function. The boundary condition at $R = 1$ is satisfied if

$$M(-\gamma, 1, \beta) + 2\gamma M(1-\gamma, 2, \beta) = 0, \tag{3.3}$$

and this transcendental equation defines the eigenvalues.

Chatwin and the earlier authors he cites investigated the high- and low-frequency asymptotic expansions of the solution (3.2) satisfying (3.3), and his conclusions are summarized in table 1. For the present work, the eigenvalues were computed directly from the defining problem (3.1) by the two methods described in §2. The real and imaginary parts of the first 7 eigenvalues as a function of $\log_{10}(\Omega)$ are displayed in

Frequency parameter $\Omega = \omega a^2/\kappa$	$\Omega \ll 1$	$\Omega \gg 1$
	$\lambda_0(\Omega) = 1 - \frac{1}{48}\mathrm{i}\Omega - \frac{1}{1920}\Omega^2 + O(\Omega^3)$	
Eigenvalues	$\lambda_p(\Omega) \approx -\left(\frac{8\mathrm{i}}{9\Omega}\right)(3p-2)^2 \quad (p \geqslant 1)$	$\lambda_p(\Omega) \approx \frac{1}{2} + (2p+1)/(\mathrm{i}\Omega)^{\frac{1}{2}} \quad (p \geqslant 0)$
Eigenfunctions	$\psi_0(R,\Omega) = 1 + \frac{1}{24}\mathrm{i}\Omega(1 - 6R^2 + 3R^4) + O(\Omega^2)$	$\psi_p(R,\Omega) \approx \exp\{-\frac{1}{2}(\mathrm{i}\Omega)^{\frac{1}{2}}R\} \times M(-p, 1, (\mathrm{i}\Omega)^{\frac{1}{2}}R^2)$
	$\psi_p(R,\Omega)$ not given for $p \geqslant 1$	
Transport speed $U/\mathrm{Re}(\lambda_0)$	U (discharge speed)	$2U$ (i.e. maximum speed)
Decay distance $-U/\omega\,\mathrm{Im}(\lambda_0)$	$48(Ua^2/\kappa)\Omega^{-2}$	$\sqrt{2}\,(Ua^2/\kappa)\Omega^{-\frac{1}{2}}$

TABLE 1. Summary of Chatwin's results concerning dispersion in Poiseuille flow in a circular pipe of radius a, discharge speed U, molecular diffusivity κ, frequency parameter $\Omega = \omega a^2/\kappa$, axial diffusion neglected

figures 1 (a, b). There are several noteworthy features of the computed eigenvalues. The first feature (which is not shown on figures 1 a, b) is that there is good agreement between the computed eigenvalues and the high- and low-frequency expansions presented by Chatwin. Secondly, the eigenvalue branches $\lambda_1(\Omega)$ and $\lambda_2(\Omega)$ nearly coalesce when $\Omega \approx 32.3$. As Ω increases beyond this value, the λ_1 branch reverts to an unexceptional pattern, whilst the λ_2 branch has quite anomalous behaviour which the author was unable to deduce from high-frequency expansions. Check calculations of this 'near miss' were performed using both eigenvalue-finding techniques, very fine meshes and both computers mentioned earlier. The results of these check calculations near $\Omega = 32$ are shown in figure 2, and comparisons of the numerical results for various meshes are shown in table 2. The eigenfunctions (normalized so that $\psi_p(0,\Omega) = 1$) were also computed to check that the boundary conditions (3.1b) were satisfied. Figure 3 shows the eigenfunction corresponding to $\lambda_1(\Omega)$ at $\Omega = 1, 10, 100, 1000$; whilst figure 4 shows the eigenfunction corresponding to $\lambda_2(\Omega)$ at $\Omega = 20, 40, 60, 80$. A comparison of figures 3 and 4 shows the anomalous behaviour of the $\lambda_2(\Omega)$ branch as Ω increases: for Ω large, the eigenfunction $\Psi_2(R,\Omega)$ has bigger amplitude near $R = 1$ than near $R = 0$ as expected. The eigenfunction corresponding to the anomalous branch is strongly damped in the direction of the flow, however, since $\mathrm{Im}(\lambda_2(\Omega))$ is more negative than $\mathrm{Im}(\lambda_j(\Omega))$ for the other branches $(j \neq 2)$ for Ω large.

4. Results for plane Couette flow, $\epsilon = 0$

Suppose that a solute with constant molecular diffusivity κ is injected into plane Couette flow with the velocity profile

$$V(Y) = 1 + Y \quad (-1 < Y < 1), \tag{4.1}$$

and the effects of longitudinal molecular diffusion are ignored ($\epsilon = 0$). The frequency parameter Ω becomes $\omega a^2/\kappa$ and the eigenvalue problem (2.3) takes the form

$$\frac{\mathrm{d}^2\psi}{\mathrm{d}Y^2} = \mathrm{i}\Omega[1 - \lambda - \lambda Y]\psi, \tag{4.2a}$$

$$\frac{\mathrm{d}\psi}{\mathrm{d}Y} = 0 \quad \text{at} \quad Y = \pm 1. \tag{4.2b}$$

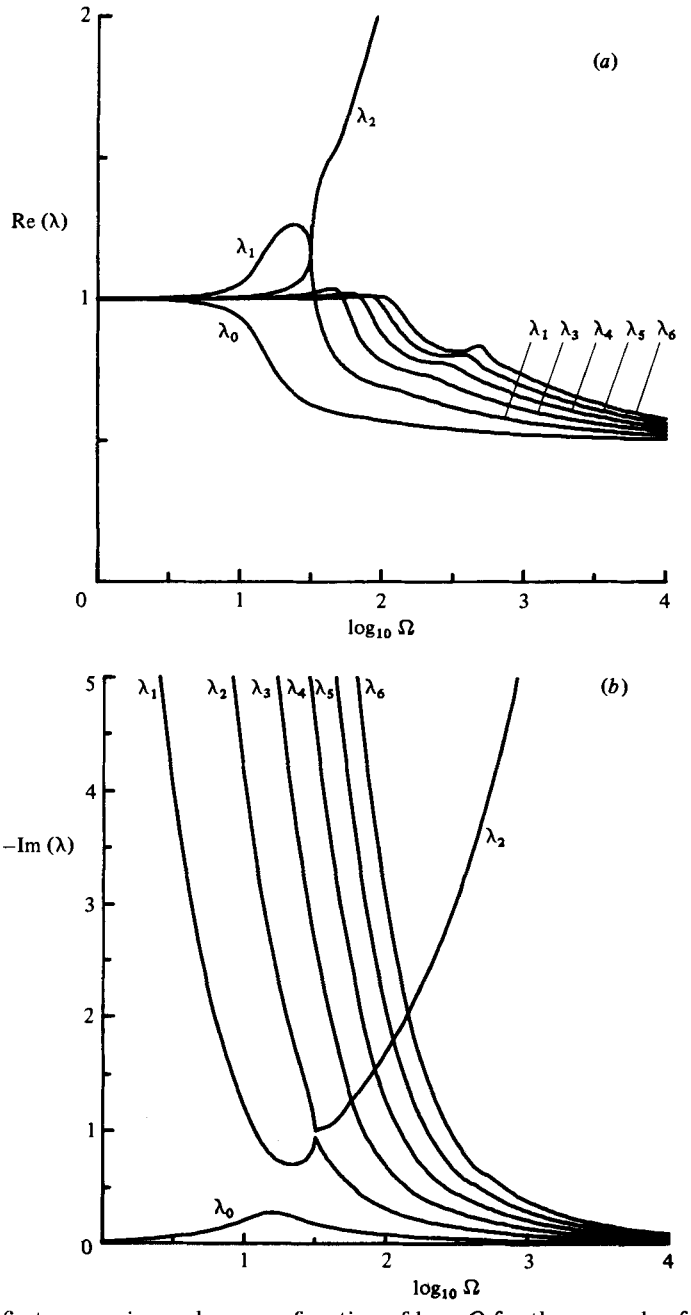

FIGURE 1. The first seven eigenvalues as a function of $\log_{10}\Omega$ for the example of §3: (*a*) real part of eigenvalues, (*b*) imaginary part of eigenvalues.

The solution to this eigenvalue problem is (Chatwin 1973*a*, p. 665)

$$\psi(Y,\Omega) = M_1 \operatorname{Ai}\left(\frac{\lambda Y+\lambda-1}{\alpha}\right) + M_2 \operatorname{Bi}\left(\frac{\lambda Y+\lambda-1}{\alpha}\right), \tag{4.3a}$$

where

$$\alpha = (-\lambda^2/\mathrm{i}\Omega)^{\frac{1}{3}}. \tag{4.3b}$$

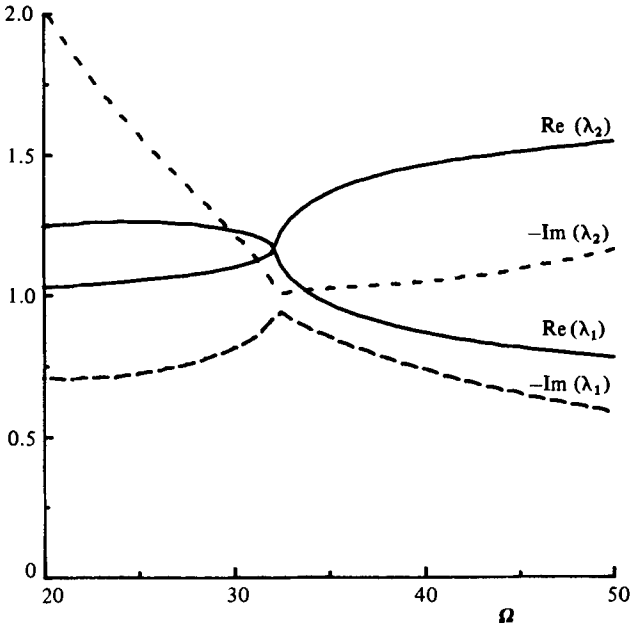

FIGURE 2. The behaviour of λ_1 and λ_2 around the point of near-coalescence.

		Central-difference method			Shooting method		
Eigenvalue	Ω	N	Re (λ)	$-$Im (λ)	N	Re (λ)	$-$Im (λ)
λ_1	31	50	1.2088	0.85471	25	1.2137	0.85126
		100	1.2125	0.85220	50	1.2137	0.85135
		200	1.2133	0.85151	100	1.2137	0.85136
		300	1.2134	0.85158	200	1.2137	0.85136
	32	50	1.1695	0.92178	25	1.1804	0.91481
		100	1.1780	0.91679	50	1.1805	0.91515
		200	1.1797	0.91541	100	1.1805	0.91517
		300	1.1799	0.91538	200	1.1805	0.91517
	33	50	1.0534	0.91430	25	1.0602	0.91907
		100	1.0582	0.91795	50	1.0599	0.91917
		200	1.0594	0.91875	100	1.0598	0.91918
		300	1.0597	0.91895	200	1.0598	0.91918
λ_2	31	50	1.1207	1.1435	25	1.202	1.1496
		100	1.1200	1.1478	50	1.1198	1.1492
		200	1.1199	1.1489	100	1.1198	1.1492
		300	1.1200	1.1491	200	1.1198	1.1492
	32	50	1.1607	1.0417	25	1.1543	1.0510
		100	1.1553	1.0482	50	1.1538	1.0505
		200	1.1541	1.0500	100	1.1538	1.0504
		300	1.1542	1.0501	200	1.1538	1.0504
	33	50	1.2772	1.0178	25	1.2749	1.0151
		100	1.2755	1.0156	50	1.2749	1.0148
		200	1.2750	1.0150	100	1.2749	1.0147
		300	1.2750	1.0151	200	1.2749	1.0147

TABLE 2. Comparison of calculated values for λ_1 and λ_2 at $\Omega = 31, 32, 33$. The calculations for both methods were performed on a PDP 11/34 minicomputer

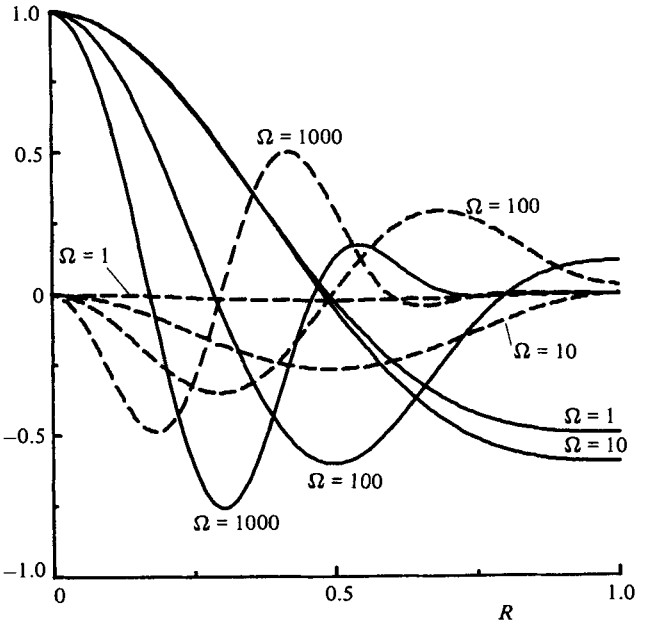

FIGURE 3. The eigenfunction $\psi_1(R, \Omega)$ for $\Omega = 1, 10, 100, 1000$ normalized so that $\psi_1(0, \Omega) = 1$: ——, real part; – – –, imaginary part.

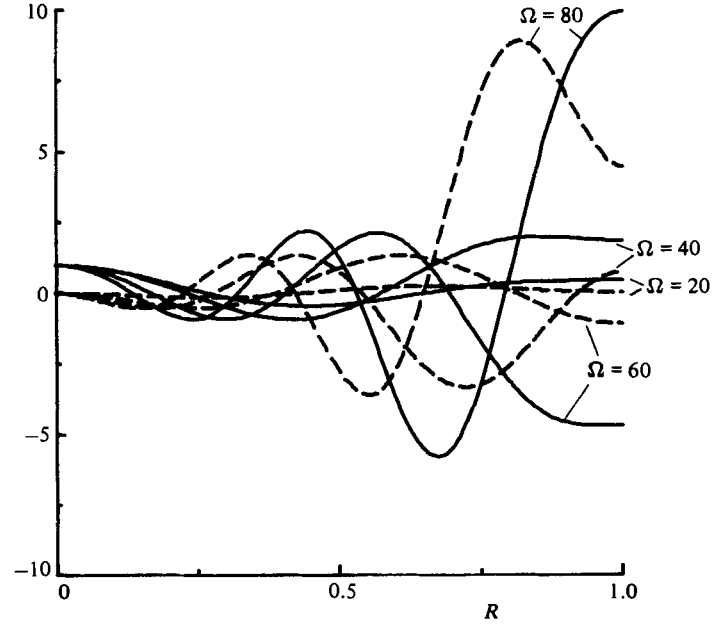

FIGURE 4. The eigenfunction $\psi_2(R, \Omega)$ for $\Omega = 20, 40, 60, 80$ normalized so that $\psi_2(0, \Omega) = 1$: ——, real part; – – –, imaginary part.

Here Ai, Bi are the Airy functions, and M_1, M_2 are non-zero constants. The boundary conditions (4.2*b*) give the condition

$$\mathrm{Ai}'\left(\frac{2\lambda-1}{\alpha}\right)\mathrm{Bi}'\left(\frac{-1}{\alpha}\right) = \mathrm{Ai}'\left(\frac{-1}{\alpha}\right)\mathrm{Bi}'\left(\frac{2\lambda-1}{\alpha}\right), \tag{4.4}$$

which defines the eigenvalues. Chatwin was again able to make low- and high-frequency expansions of the solutions, and a summary of his conclusions is given in table 3.

For the present work, the eigenvalues of (4.2) were computed directly and the real and imaginary parts of the first 7 eigenvalues as a function of $\log_{10}(\Omega)$ are shown in figure 5(*a*, *b*). These eigenvalues also have a 'near miss' for Ω near 10, and the λ_2 branch has anomalous behaviour for larger values of Ω. The eigenfunctions were also calculated to check that the boundary conditions were indeed satisfied on the anomalous branch. These calculations, whose results are not presented here, show large-amplitude solutions for $\psi_2(Y, \Omega)$ near $Y = -1$, particularly for Ω greater than about 20. For large values of Ω, all the other $\Psi_p(Y, \Omega)$ are confined in a region of thickness $a\Omega^{-\frac{1}{3}}$ near $Y = 1$ in accordance with Chatwin's conclusions. Again the anomalous branch is more strongly damped than the other branches for Ω large, and, again, there is fair to good agreement between the numerical calculations and Chatwin's asymptotic results.

5. Results for a model of turbulent channel flow, $\epsilon = 0$

The eigenvalue problem (2.3) is solved numerically in this section for the case when the basic flow is an idealized model of turbulent channel flow in the channel $0 < y < a$. In this case, the variables K and V are given by (Fischer *et al.* 1979, §5.1.1.1)

$$K(Y) = 6Y(1-Y), \quad V(Y) = 1 + \frac{u^*}{U\kappa}(1+\ln Y) \quad (0 < Y < 1), \tag{5.1}$$

in which u^* is the friction velocity, U is the discharge speed, κ is von Kármán's constant (approximately 0.4), and the parameter Ω becomes $\Omega = 6\omega a/\kappa u^*$ (since $D = \frac{1}{6}\kappa a u^*$). As Chatwin (1970) points out, there are severe faults with the representations (5.1): there is no firm justification for the use of Reynolds' analogy which gives $K(Y)$ (but see Fischer *et al.* 1979, §5.1.1.1), the form for $V(Y)$ neglects the important viscous sublayer (see Chatwin 1973*b*), turbulent flow in a channel is not two-dimensional, and the turbulent-diffusion process is not isotropic. (Of course, if longitudinal turbulent diffusion is neglected, so that $\epsilon = 0$, the fact that (5.1) does not correctly describe longitudinal diffusion is irrelevant.) The theory also predicts results that differ by orders of magnitude from results in natural streams and watercourses (see Fischer *et al.* 1979, §5.2.1). Nonetheless, the model has been widely studied by engineers and is certainly important for pedagogic reasons.

If longitudinal turbulent diffusion is neglected, so that $\epsilon = 0$, the eigenvalue problem (2.3) now becomes

$$\frac{\mathrm{d}}{\mathrm{d}Y}\left(6Y(1-Y)\frac{\mathrm{d}\psi}{\mathrm{d}Y}\right) = \mathrm{i}\Omega\left[1-\lambda\left(1+\frac{u^*}{U\kappa}(1+\ln Y)\right)\right]\psi \quad (0 < Y < 1), \tag{5.2a}$$

$$6Y(1-Y)\frac{\mathrm{d}\psi}{\mathrm{d}Y} = 0 \quad \text{at} \quad Y = 0, 1 \tag{5.2b}$$

which is equivalent to

$$\psi, \frac{\mathrm{d}\psi}{\mathrm{d}Y} \text{ finite} \quad \text{at} \quad Y = 0, 1. \tag{5.2c}$$

Frequency parameter $\Omega = \omega a^2/\kappa$	$\Omega \ll 1$	$\Omega \gg 1$
Eigenvalues	$\lambda_0 = 1 - \frac{2}{15}i\Omega + O(\Omega^2)$ $\lambda_p = -\dfrac{9i\pi^2 p^2}{32\Omega} \quad (p \geqslant 1)$	$\lambda_p(\Omega) \approx \frac{1}{2} + \frac{1}{2}\left(\dfrac{3\pi}{16}\right)^{\frac{2}{3}}\left(\dfrac{1}{i\Omega}\right)^{\frac{1}{3}}(4p+1)^{\frac{2}{3}} \quad (p \geqslant 0)$
Eigenfunctions	Not presented	$\psi_p(Y,\Omega) \approx \mathrm{Ai}[(1-Y)(\frac{1}{2}i\Omega)^{\frac{1}{3}} - (\frac{3}{8}\pi(4p+1))^{\frac{2}{3}}] \quad (p \geqslant 0)$
Transport speed $U/\mathrm{Re}(\lambda_0)$	U (i.e. discharge speed)	$2U$ (i.e. maximum speed)
Decay distance $-U/\omega\,\mathrm{Im}(\lambda_0)$	$\frac{15}{2}(Ua^2/\kappa)\,\Omega^{-2}$	$4(Ua^2/\kappa)\,(\frac{3}{16}\pi)^{-\frac{2}{3}}\Omega^{-\frac{1}{3}}$

TABLE 3. Summary of Chatwin's results concerning dispersion in plane Couette flow in a channel of width $2a$, discharge speed U, molecular diffusivity κ, frequency parameter $\Omega = \omega a^2/\kappa$, longitudinal diffusion neglected

In this case, the numerical schemes described in §2 require minor changes to allow for the boundary condition (5.2*c*). The altered computer program was checked by comparing the numerical results with $u^*/U\kappa = 0$ with an analytic solution which is now presented for that case. With $u^*/U\kappa = 0$ and with the substitution $\xi = 2Y - 1$, the eigenvalue problem (5.2*a*, *c*) becomes

$$\frac{\mathrm{d}}{\mathrm{d}\xi}\left((1-\xi^2)\frac{\mathrm{d}\psi}{\mathrm{d}\xi}\right) - \tfrac{1}{6}i\Omega(1-\lambda)\psi = 0, \tag{5.3a}$$

$$\psi, \frac{\mathrm{d}\psi}{\mathrm{d}\xi} \text{ finite} \quad \text{at} \quad \xi = \pm 1. \tag{5.3b}$$

The solutions of this problem are the Legendre polynomials $P_n(\xi)$, and the eigenvalues are given by $-\frac{1}{6}i\Omega(1-\lambda) = n(n+1)$ so that

$$\lambda = 1 - 6in(n+1)/\Omega. \tag{5.4}$$

The actual value of $u^*/U\kappa$ for laboratory experiments in rectangular open channels with smooth sides typically lies in the range 0.15–0.35 (Fischer *et al.* 1979, table 5.1). The eigenvalue problem (5.2) was therefore solved numerically with the values 0.2 and then 0.3 for $u^*/U\kappa$. The results, which are displayed in figures 6(*a*, *b*) and 7(*a*, *b*), do not show the anomalous eigenvalue behaviour observed in the previous two examples. Table 4 contains a summary of the asymptotic behaviour of the eigenvalues at low and high frequencies. This table is compiled from the numerical results and from Chatwin's (1973*a*) predictions.

A comparison of figures 6(*a*), 7(*a*) shows that, as $u^*/U\kappa$ is increased from 0.2 to 0.3, there are modest increases in $\mathrm{Re}(\lambda_p)$ at low frequencies (except for the λ_0 branch, which is unchanged) and decreases in $\mathrm{Re}(\lambda_p)$ at high frequencies. (The concentration pattern is transported downstream at speed $U/\mathrm{Re}(\lambda_p)$.) Figures 6(*b*), 7(*b*) show that the main features of $\mathrm{Im}(\lambda_p)$, $p \geqslant 0$, (and hence the decay distances) as functions of Ω are essentially unaltered by the change in $u^*/U\kappa$. It is noted, however, that the curves for $\mathrm{Re}(\lambda_p)$ and $\mathrm{Im}(\lambda_p)$ have more 'wiggles' (i.e. vary more rapidly with Ω) when $u^*/U\kappa$ is 0.2 rather than 0.3.

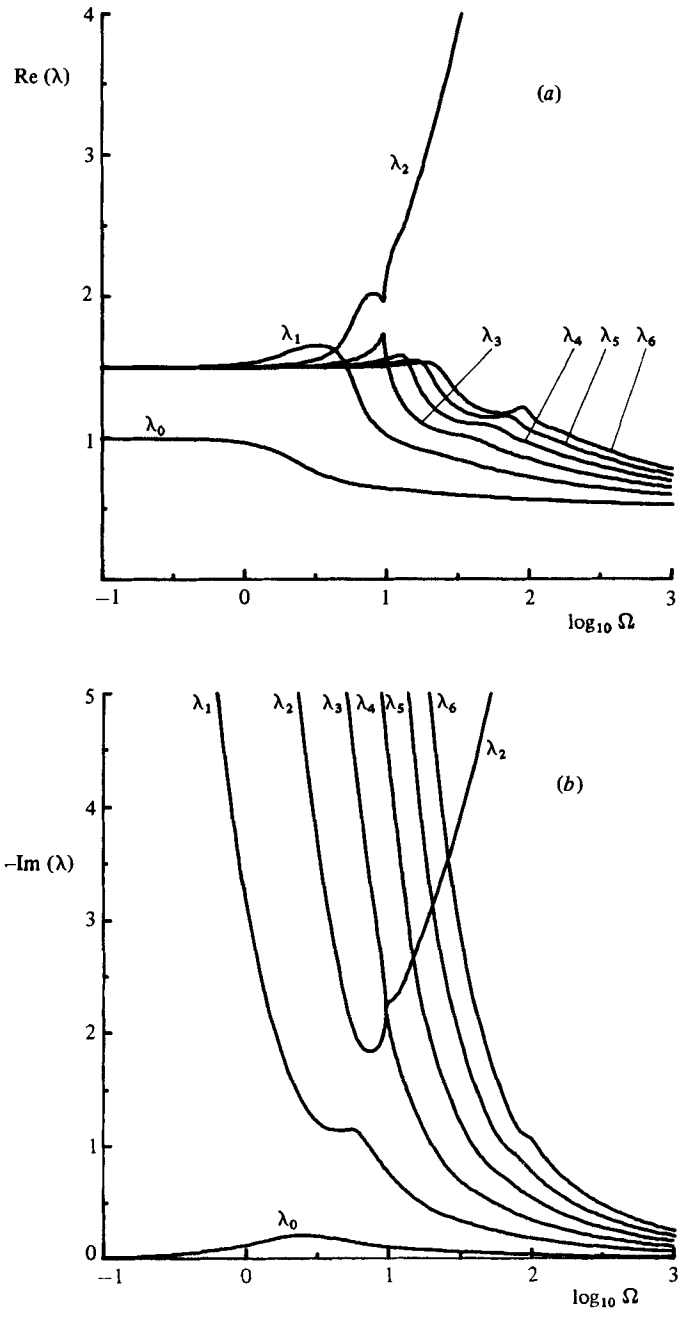

FIGURE 5. The first seven eigenvalues as a function of $\log_{10}\Omega$ for the example of §4: (*a*) real part of eigenvalues, (*b*) imaginary part of eigenvalues.

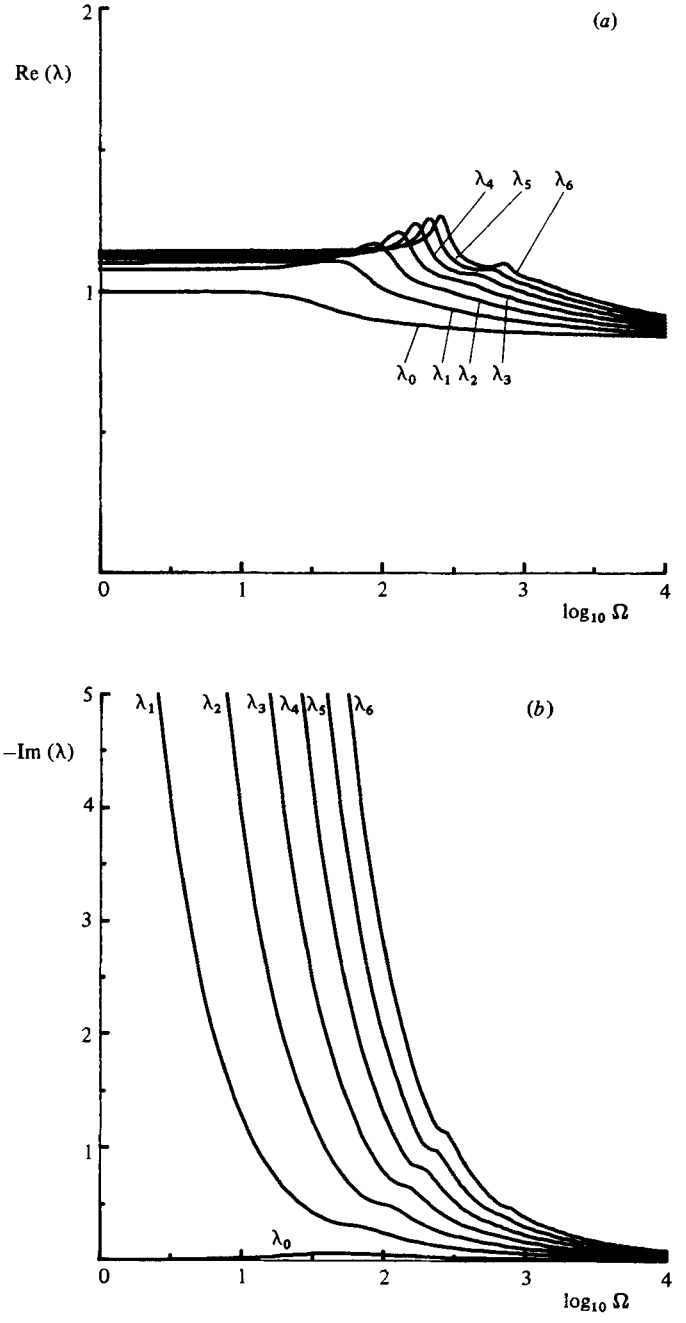

FIGURE 6. The first seven eigenvalues as a function of $\log_{10}\Omega$ for the example of §5 (turbulence parameter $u^*/U\kappa = 0.2$): (*a*) real part of eigenvalues, (*b*) imaginary part of eigenvalues.

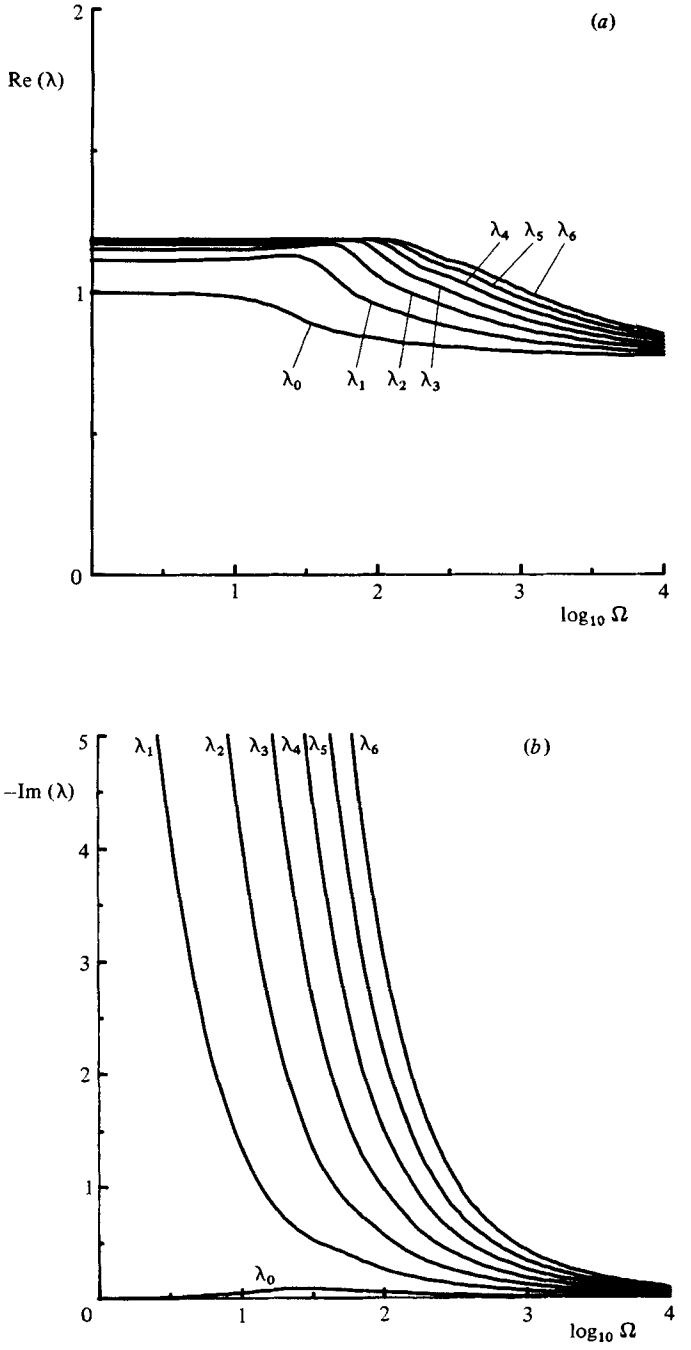

FIGURE 7. The first seven eigenvalues as a function of $\log_{10}\Omega$ for the example of §5 (turbulence parameter $u^*/U\kappa = 0.3$): (*a*) real part of eigenvalues, (*b*) imaginary part of eigenvalues.

	Frequency parameter $\Omega = 6\omega a/\kappa u^*$	$\Omega \ll 1$	$\Omega \gg 1$
	Eigenfunctions	Oscillatory over channel	Confined to a thick region near $Y = 1$
Turbulence parameter $u^*/U\kappa = 0.2$	Transport speed $U/\mathrm{Re}\,(\lambda_0)$	U (i.e. discharge speed)	$\approx U(1+0.3\ln 2)$ (i.e. maximum speed)
	Decay distance $-U/\omega\,\mathrm{Im}\,(\lambda_0)$	$89.1a\Omega^{-2}\kappa^{-2}\,(0.2)^{-3}$	$\dfrac{6a}{\kappa^2(u^*/U\kappa)}\{\Omega\,\mathrm{Im}\,(\lambda_0)\}^{-1}$
Turbulence parameter $u^*/U\kappa = 0.3$	Transport speed $U/\mathrm{Re}\,(\lambda_0)$	U (i.e. discharge speed)	$\approx U(1+0.3\ln 2)$ (i.e. maximum speed)
	Decay distance $-U/\omega\,\mathrm{Im}\,(\lambda_0)$	$89.1a\Omega^{-2}\,\kappa^{-2}\,(0.3)^{-3}$	$\dfrac{6a}{\kappa^2(u^*/U\kappa)}\{\Omega\,\mathrm{Im}\,(\lambda_0)\}^{-1}$

TABLE 4. Summary of results for dispersion in a model of turbulent flow in a channel of depth a, discharge speed U, frequency parameter $\Omega = 6\omega a/\kappa u^*$ (κ is von Kármán's constant, u^* is the friction velocity), longitudinal turbulent diffusion neglected. The low-frequency eigenvalue expansion used is $\lambda_0 = 1 - 0.0673\mathrm{i}\Omega(u^*/U\kappa)^2 + O(\Omega^2)$, which is derived from results of Chatwin (1973, equation (2.19)) and Elder (1959).

6. Theoretical implications of weak longitudinal diffusion, $0 < \epsilon \ll 1$

In this section, weak longitudinal diffusion is retained in the eigenvalue problem (2.3), and approximations to the eigenvalues and eigenfunctions are calculated using a regular perturbation expansion in ϵ. The analysis is taken far enough to determine $O(\epsilon^2)$ corrections to the eigenvalues. The perturbation calculation in ϵ has application to problems in which ϵ is small, and these problems are common in the dispersion of matter in laminar flows in liquids (Chatwin 1973*a*, p. 659).

Consider therefore the eigenvalue problem (2.3) with $0 < \epsilon \ll 1$, where it is assumed that the corresponding problem with $\epsilon = 0$ possesses a discrete set of complex eigenvalues $\{\lambda_{p0}\}$ and a corresponding complete set of eigenfunctions $\{\psi_{p0}\}$. Suppose that the eigenvalues and eigenfunctions for $\epsilon > 0$ have the expansions

$$\lambda_p(\Omega, \epsilon) = \lambda_{p0}(\Omega) + \epsilon\lambda_{p1}(\Omega) + \epsilon^2\lambda_{p2}(\Omega) + \ldots, \tag{6.1a}$$

$$\psi_p(Y, Z, \Omega, \epsilon) = \psi_{p0}(Y, Z, \Omega) + \epsilon\psi_{p1}(Y, Z, \Omega) + \epsilon^2\psi_{p2}(Y, Z, \Omega) + \ldots, \tag{6.1b}$$

where it is found from (2.3) that ψ_{p0}, ψ_{p1} and ψ_{p2} are solutions of

$$\boldsymbol{\nabla}\cdot(K\boldsymbol{\nabla}\psi_{p0}) = \mathrm{i}\Omega(1 - \lambda_{p0} V)\psi_{p0}, \tag{6.2a}$$

$$\boldsymbol{\nabla}\cdot(K\boldsymbol{\nabla}\psi_{p1}) = \mathrm{i}\Omega[(1 - \lambda_{p0} V)\psi_{p1} + (-\lambda_{p1} V - \mathrm{i}\lambda_{p0}^2 K)\psi_{p0}], \tag{6.2b}$$

$$\boldsymbol{\nabla}\cdot(K\boldsymbol{\nabla}\psi_{p2}) = \mathrm{i}\Omega[(1 - \lambda_{p0} V)\psi_{p2} + (-\lambda_{p1} V - \mathrm{i}\lambda_{p0}^2 K)\psi_{p1} + (-\lambda_{p2} V - 2\mathrm{i}\lambda_{p0}\lambda_{p1} K)\psi_{p0}] \tag{6.2c}$$

under the boundary condition (2.3*b*). The solutions to (6.2*a*) are known by hypothesis, and standard (solvability) manipulations can be employed to determine λ_{p1} and λ_{p2}. Specifically, if the difference $\{\boldsymbol{\nabla}\cdot(\psi_{p0} K\boldsymbol{\nabla}\psi_{p1}) - \boldsymbol{\nabla}\cdot(\psi_{p1} K\boldsymbol{\nabla}\psi_{p0})\}$ is integrated over the cross-section of the flow, (6.2*a*, *b*) and the boundary condition (2.3*b*) give

$$\lambda_{p1} = -\frac{\mathrm{i}\lambda_{p0}^2 \iint K\psi_{p0}^2 \,\mathrm{d}S}{\iint V\psi_{p0}^2 \,\mathrm{d}S}. \tag{6.3}$$

The eigenfunction correction ψ_{p1} can be sought as a linear combination of the $\{\psi_{p0}\}$; that is,

$$\psi_{p1} = \sum_q a_{pq}\psi_{q0}, \tag{6.4}$$

where standard manipulations show that the a_{pq} are given by

$$a_{pq} = \begin{cases} \dfrac{\lambda_{p1}\iint V\psi_{p0}\psi_{q0}\,\mathrm{d}S + \mathrm{i}\lambda_{p0}^2\iint K\psi_{p0}\psi_{q0}\,\mathrm{d}S}{\mathrm{i}\Omega(\lambda_{q0} - \lambda_{p0})\iint V\psi_{q0}^2\,\mathrm{d}S} & (p \neq q), \\ \text{arbitrary} & (p = q). \end{cases} \tag{6.5}$$

These results (6.4), (6.5) for ψ_{p1} enable the second correction λ_{p2} to the eigenvalue $\lambda_p(\Omega, \epsilon)$ to be calculated: that is, the solvability condition applied to (6.2*c*) gives

$$\lambda_{p2} = -\frac{\lambda_{p1}\iint V\psi_{p1}\psi_{p0}\,\mathrm{d}S + \mathrm{i}\lambda_{p0}^2\iint K\psi_{p1}\psi_{p0}\,\mathrm{d}S + 2\mathrm{i}\lambda_{p0}\lambda_{p1}\iint K\psi_{p0}^2\,\mathrm{d}S}{\iint V\psi_{p0}^2\,\mathrm{d}S}, \tag{6.6}$$

in which λ_{p1} and ψ_{p1} are given by (6.3) and (6.4), (6.5) respectively.

The $O(\epsilon)$ correction described by (6.3) has an immediate consequence – longitudinal diffusion will produce relatively large changes in strongly damped eigenvalues. This follows since strongly damped eigenvalues have $|\lambda_{p0}|$ large, and hence λ_{p1}, which is proportional to λ_{p0}^2, will be large also. This conclusion will be verified by numerical work presented in §7.

7. Axial-diffusion effects in Poiseuille flow, $\epsilon \neq 0$

The topic of §3 is now reconsidered with axial-diffusion effects included; the eigenvalue problem governing the dispersion of the contaminant is therefore

$$\frac{1}{R}\frac{\mathrm{d}}{\mathrm{d}R}\left(R\frac{\mathrm{d}\psi}{\mathrm{d}R}\right) = \mathrm{i}\Omega\{1-2\lambda(1-R^2)-\mathrm{i}\epsilon\lambda^2\}\psi, \tag{7.1a}$$

$$\frac{\partial\psi}{\partial R} = 0 \quad \text{at} \quad R = 0, 1. \tag{7.1b}$$

In this problem, ϵ is defined by $\epsilon = \Omega(\kappa/Ua)^2 = (\omega a^2/\kappa)(\kappa/Ua)^2$ and is a measure of the importance of axial diffusion compared to axial convection effects. The problem (7.1) was solved numerically using the techniques described in §2, and the results were checked for very small ϵ using the $O(\epsilon)$ correction obtained in §6. This confirmed the tangents in the (λ, ϵ)-plane to the solutions for $\lambda(\Omega, \epsilon)$ at $\epsilon = 0$.

The eigenvalues of problem (7.1) are displayed in figures 8(*a*, *b*) as functions of $\log_{10}(\Omega)$ for $\epsilon = 0, 0.1, 0.2, 0.5, 1.0$, and a brief tabulation of some of the computations is given in table 5. The figures show that the anomalous eigenvalue branches persist up to $\epsilon = 1.0$, although the anomalous branch becomes less damped at high frequencies as ϵ is increased. Axial diffusion has a marked effect on the transport speed at low frequencies for all eigenvalues and, in agreement with the observations of §6, this effect is most noticeable for the eigenmodes with $p \geqslant 1$ which are strongly damped. An increase in axial diffusion means that the concentration pattern corresponding to all eigenmodes is transported slower. Axial diffusion increases the damping in the first eigenmode ($p = 0$), particularly at low frequencies, but reduces the damping of all the other eigenmodes at all but very high frequencies.

8. Discussion

The eigenvalue problem that has been investigated in this paper underlies all experiments on the dispersion of solutes by fluids in parallel flow. That is, it is experimentally impossible to inject a solute into a fluid in other than a time-dependent fashion and so, in every application, the eigenvalue problem is present whether it is acknowledged or not by investigators. Thus it is surprising that the problem has received as little attention as it has in the past.

The eigenvalue problem is unusual for various reasons which have been presented throughout the paper and are now summarized. The problem is not self-adjoint because complex coefficients are involved and because the eigenvalue enters it nonlinearly. (This last fact could be obviated by Fourier-transforming the problem in x and not t, but this would be appropriate for dispersion from an initial distribution which is known for all x, and this is not the usual *experimental* condition.) The eigenvalue problem has singular perturbation aspects in that, for Ω large, most of the eigenfunctions are confined within a region $a\Omega^{-\beta}$ of the position in the cross-section where the fluid speed is largest. Here the index β varies from problem to problem – it

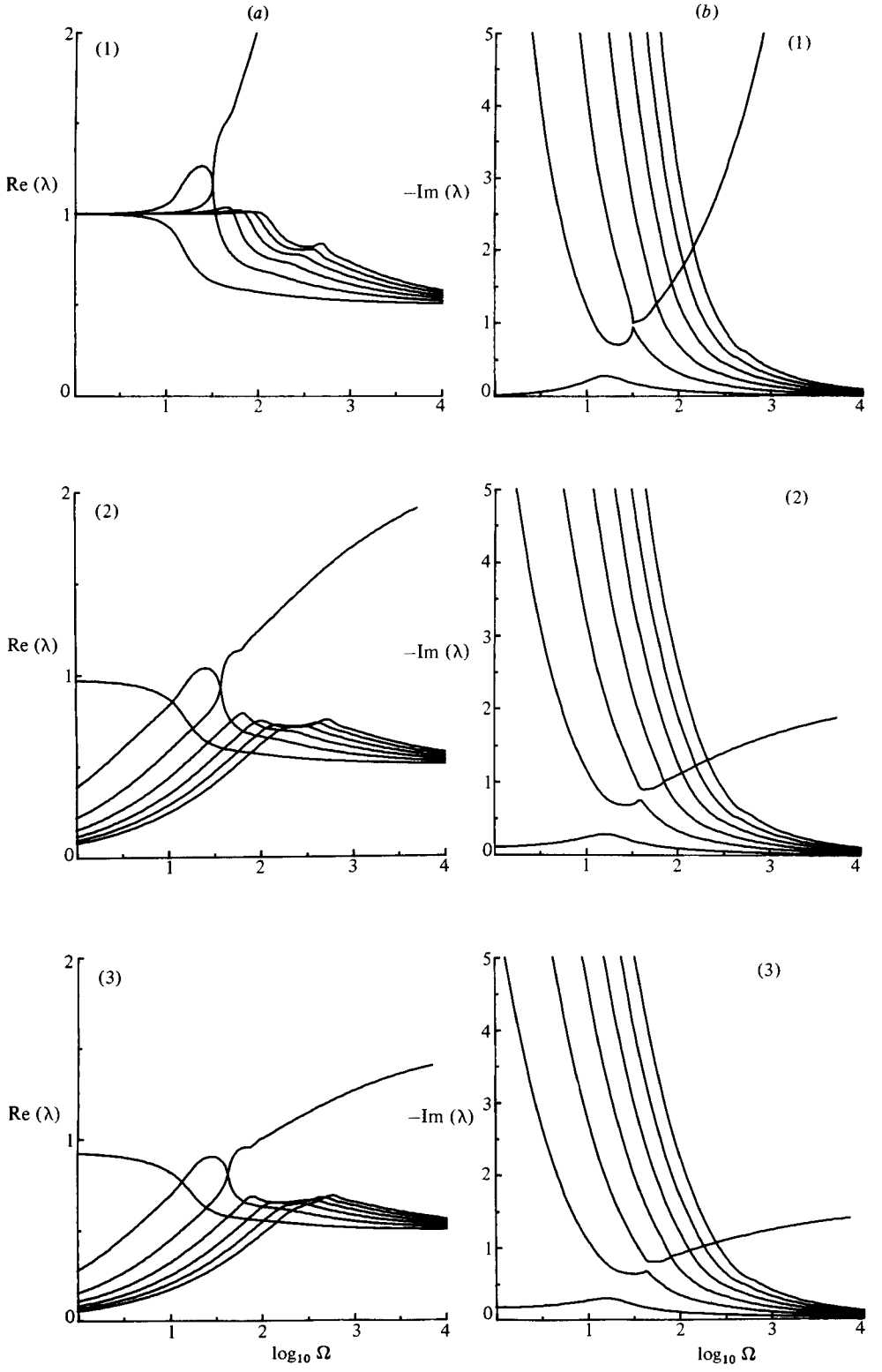

FIGURE 8. For caption see facing page.

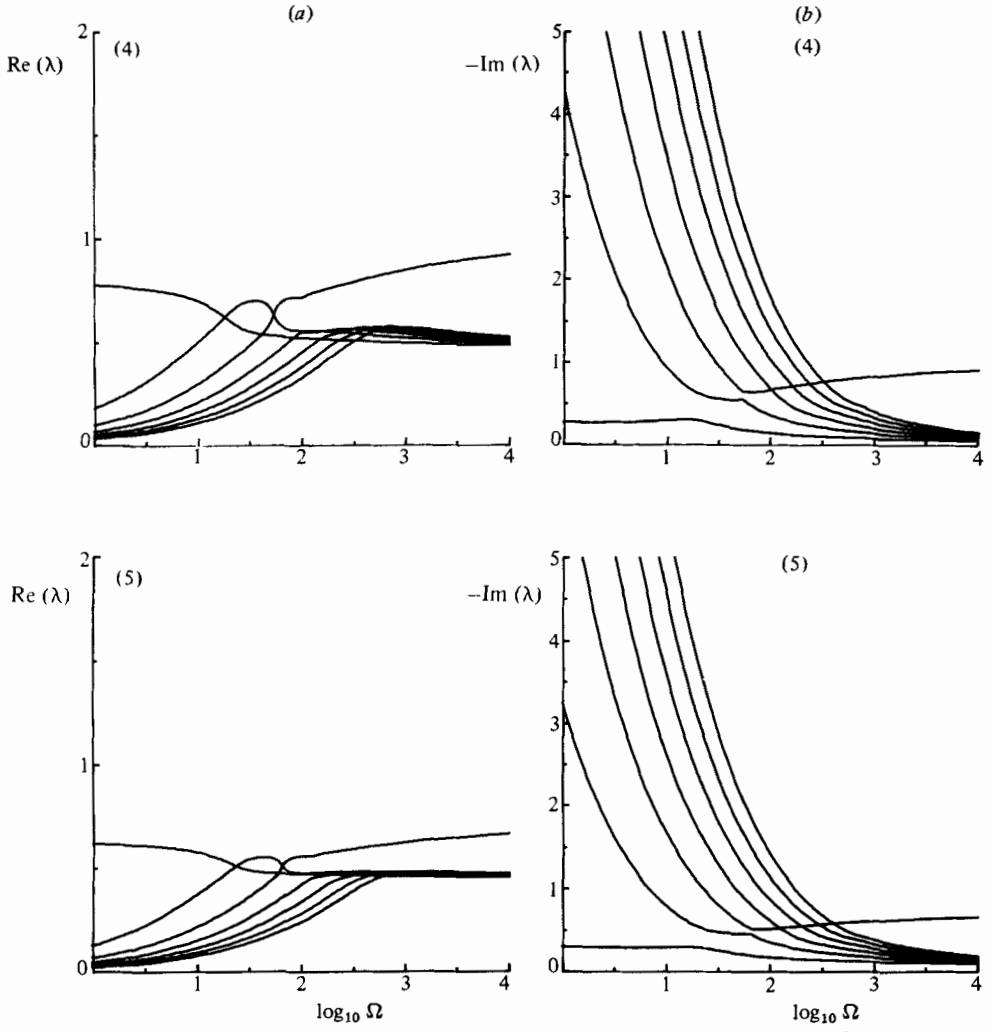

FIGURE 8. The first seven eigenvalues as a function of $\log_{10}\Omega$ and ϵ for the example of §7: (*a*) real part of eigenvalues, (*b*) imaginary part of eigenvalues: (1) $\epsilon = 0$; (2) 0.1; (3) 0.2; (4) 0.5; (5) 1.0.

was $\frac{1}{4}$ and $\frac{1}{3}$ for the problems of §§3 and 4 respectively. Moreover, the eigenvalue problem has regular perturbation aspects in that, in many cases, the effect of longitudinal diffusion is given by a regular expansion in the small parameter ϵ.

When longitudinal diffusion is completely neglected so that ϵ in (2.3) is set equal to zero, one eigenvalue branch in two out of the three problems studied showed anomalous and unexpected behaviour. It is conjectured that some higher eigenvalue branches in all of the problems might also have the anomalous behaviour. The most immediate conclusion that can be drawn from the numerical results is that the eigenvalue structure is significantly richer than is suggested by the asymptotic results for small and large Ω presented by Chatwin. The peculiar near-coalescence of the eigenvalue branches in the Poiseuille and Couette flow cases brings bifurcation theory to mind, and it is possible that the effects may be associated with a singularity lying close to the real axis in the complex Ω-plane. The anomalous eigenvalue branches

		Lowest eigenmode λ_0	
		Re (λ)	$-$Im (λ)
$\Omega = 1$	$\epsilon = 0$	0.99948	0.020840
	0.1	0.97368	0.11313
	0.2	0.92577	0.18211
	0.5	0.77721	0.27530
	1.0	0.61991	0.30033
$\Omega = 10$	$\epsilon = 0$	0.93525	0.21302
	0.1	0.87353	0.25995
	0.2	0.82034	0.27258
	0.5	0.70009	0.30032
	1.0	0.57687	0.30157
$\Omega = 100$	$\epsilon = 0$	0.56996	0.080386
	0.1	0.56301	0.096590
	0.2	0.55458	0.11137
	0.5	0.52423	0.14624
	1.0	0.47234	0.17836
$\Omega = 1000$	$\epsilon = 0$	0.52235	0.023372
	0.1	0.52008	0.037087
	0.2	0.51645	0.050277
	0.5	0.49935	0.084855
	1.0	0.46179	0.12352
			λ_1
		Re (λ)	$-$Im (λ)
$\Omega = 1$	$\epsilon = 0$	1.0004	12.834
	0.1	0.38501	7.4834
	0.2	0.28171	6.0185
	0.5	0.18189	4.3017
	1.0	0.12950	3.2457
$\Omega = 10$	$\epsilon = 0$	1.0542	1.2277
	0.1	0.82525	1.1713
	0.2	0.69502	1.1019
	0.5	0.50373	0.94528
	1.0	0.37448	0.79417
$\Omega = 100$	$\epsilon = 0$	0.69001	0.31368
	0.1	0.66063	0.33150
	0.2	0.63237	0.34377
	0.5	0.55987	0.35955
	1.0	0.47615	0.35660
$\Omega = 1000$	$\epsilon = 0$	0.56678	0.076384
	0.1	0.56024	0.092347
	0.2	0.55221	0.10697
	0.5	0.52293	0.14178
	1.0	0.47210	0.17434

TABLE 5. Computed values for $\lambda_0(\Omega, \epsilon)$ and $\lambda_1(\Omega, \epsilon)$ at $\Omega = 1$, 10, 100, 1000 and $\epsilon = 0$, 0.1, 0.2, 0.5, 1.0 for the example of §7. The transport speed of the eigenmode is $U/\mathrm{Re}\,(\lambda)$ and its decay distance in the downstream direction is $-aP/\Omega\,\mathrm{Im}\,(\lambda)$.

are relatively strongly damped compared to other branches and therefore are not particularly important physically; it would presumably be difficult to detect their effects experimentally. It should be stressed that this peculiar behaviour is an artifact of the problem and not of the computational methods. Another important unanswered question is why the almost-coalescing behaviour does not occur in the model for turbulent channel flow? It is possible that anomalous behaviour occurs for those singular eigenvalue problems in which the velocity profile vanishes at the walls. This possibility would appear to be more plausible since the author (Barton 1983) has recently shown that anomalous eigenvalue behaviour also occurs when the basic flow is plane Poiseuille flow which vanishes at the boundaries.

The Fourier-decomposition method has further complications when longitudinal diffusion is included. Then, orthogonality of the eigenfunctions is lost, so that fitting constants as in (2.7) becomes more difficult. Also, the occurrence of longitudinal diffusion means that simple estimates of the transport speed and damping rates of the concentration pattern through (2.8*a*, *b*) are no longer possible. Another important result is that small amounts of longitudinal diffusion cause relatively large changes in the eigenvalues, and hence in the transport speed and decay distance of the concentration pattern. The effect is most pronounced for strongly damped eigenmodes. This theoretical prediction which was made in §6 was confirmed in §7 for the case of dispersion from a harmonically varying source in Poiseuille flow. The importance of axial diffusion can be seen from the eigenvalues λ_0 and λ_1 listed in table 5 for $\Omega = 1$, 10, 100, 1000 and $\epsilon = 0$, 0.1, 0.2, 0.5, 1.0. (For any eigenmode, the transport speed is given by $U/\mathrm{Re}\,(\lambda)$ and the decay distance in the downstream direction by

$$\frac{-U}{\omega\,\mathrm{Im}\,(\lambda_p)} = -\frac{Ua^2/\Omega D}{\mathrm{Im}\,(\lambda_p)} = -\frac{aP/\Omega}{\mathrm{Im}\,(\lambda_p)},$$

where $P = Ua/D$ is the Péclet number of the flow.) In many cases, a relatively small change in ϵ produces a pronounced change in either $\mathrm{Re}\,(\lambda)$ or $\mathrm{Im}\,(\lambda)$. For example, at $\Omega = 1$, changing ϵ from 0 to 0.1 changes $\mathrm{Im}\,(\lambda_0)$ by a factor of 5.4 and $\mathrm{Re}\,(\lambda_1)$ by a factor of 2.6.

The conclusion to be drawn from the previous paragraphs is that it may not be desirable or optimal to solve the time-dependent injection problem by Fourier decomposition in time. The Fourier approach does of course give relatively straightforward results for the lowest eigenmode and for asymptotically small or large values of Ω, but the complexity of the associated non-standard eigenvalue problem makes it worthwhile to consider other methods of solution. For this reason, the approach adopted by Plumb *et al.* (1983) is now described briefly. For a general problem, suppose that the input strength at $x = 0$,

$$C(0, Y, Z, t) = f(t)g(Y, Z), \tag{8.1}$$

is written as

$$C(0, Y, Z, t) = \int_{-\infty}^{t} \mathrm{d}\tau \iint_{\text{cross-section}} \mathrm{d}\xi\,\mathrm{d}\eta f(\tau)\, g(\xi, \eta)\, \delta(t-\tau)\, \delta(\xi - Y)\, \delta(\eta - Z). \tag{8.2}$$

The solution is then given by convolving the solution for dispersion from a δ-function source at $t = \tau$, $\xi = Y$, $\eta = Z$ with the functions $f(\tau)\, g(\xi, \eta)$. Since the dispersion from δ-function sources is becoming ever-better understood, this approach may be more

practical than the Fourier decomposition approach in some applications. Thus for the experiments of Plumb *et al.* (1983) on dispersion of mixtures of gases, neither large- nor small-frequency expansions were applicable and there was significant axial diffusion. Plumb *et al.* therefore adopted the convolution approach in preference to the Fourier-decomposition approach to analyse their observations. (It would presumably be a valuable exercise to refit the data of Plumb *et al.* using the Fourier decomposition approach for comparison with the results obtained using (8.1, 8.2); the author may attempt this in the future.) The convolution approach is particularly suitable if large-time results are required because the large-time asymptotic solution for dispersion from a δ-function source is very well understood (Chatwin 1970). It is noted in conclusion that the convolution approach to dispersion problems with time-dependent injection has also been proposed and discussed by Gill & Sankara-subramanian (1972).

The author would like to thank Dr P. C. Chatwin for his helpful comments on a preliminary draft of this paper.

REFERENCES

ANDREWS, A. L. 1974 Eigenvalue problems with nonlinear dependence on the eigenvalue parameter. A bibliography. *Tech. Rep., Dept Maths, La Trobe University, Bundoora, Australia 3083.*

ARIS, R. 1956 On the dispersion of a solute in a fluid flowing through a tube. *Proc. R. Soc. Lond.* A **235**, 67–77.

BARTON, N. G. 1983 Further results on the dispersion of solute from a time-dependent source. In *Proc. 8th Australasian Fluid Mech. Conf.* Inst. of Engrs, Australia (to appear).

BRINKMAN, H. C. 1950 Heat effects in capillary flow I. *Appl. Sci. Res.* **A2**, 120–124.

BOYCE, W. E. & DI PRIMA, R. C. 1977 *Elementary Differential Equations and Boundary Value Problems*, 3rd edn. Wiley.

CARRIER, G. F. 1956 On diffusive convection in tubes. *Q. Appl. Maths* **14**, 108–112.

CHATWIN, P. C. 1970 The approach to normality of the concentration distribution of a solute in a solvent flowing along a straight pipe. *J. Fluid Mech.* **43**, 321–352.

CHATWIN, P. C. 1973*a* On the longitudinal dispersion of dye whose concentration varies harmonically with time. *J. Fluid Mech.* **58**, 657–667.

CHATWIN, P. C. 1973*b* A calculation illustrating the effects of the viscous sub-layer on longitudinal dispersion. *Q. J. Mech. Appl. Maths* **26**, 427–439.

ELDER, J. W. 1959 The dispersion of marked fluid in turbulent shear flow. *J. Fluid Mech.* **5**, 544–560.

FISCHER, H. B., IMBERGER, J., LIST, E. J., KOH, R. C. Y. & BROOKS, N. H. 1979 *Mixing in Inland and Coastal Waters.* Academic.

GILL, W. M. & SANKARASUBRAMANIAN, R. 1970 Exact analysis of unsteady convective diffusion. *Proc. R. Soc. Lond.* A **316**, 341–350.

GILL, W. M. & SANKARASUBRAMANIAN, R. 1972 Dispersion of non-uniformly distributed time-variable continuous sources in time-dependent flow. *Proc. R. Soc. Lond.* A **327**, 191–208.

HOWARD, C. J. 1976 Kinetic measurements using flow tubes. *J. Phys Chem.* **83**, 3–8.

PAINE, J. W. & ANDERSSEN, R. S. 1980 Uniformly valid approximation of eigenvalues of Sturm–Liouville problems in geophysics. *Geophys. J. R. Astr. Soc.* **63**, 441–465.

PHILIP, J. R. 1963*a* The theory of dispersal during laminar flow in tubes, I. *Austral. J. Phys.* **16**, 287–299.

PHILIP, J. R. 1963*b* The theory of dispersal during laminar flow in tubes, II. *Austral. J. Phys.* **16**, 300–310.

PLUMB, I. C., RYAN, K. R. & BARTON, N. G. 1983 A method for the measurement of diffusion coefficients of labile gas phase species: the diffusion coefficient of $O(^3P)$ in He at 294 K. *Intl J. Chem. Kinetics* (to appear).

SMITH, R. 1981 A delay-diffusion description for contaminant dispersion. *J. Fluid Mech.* **105**, 469–486.

SOUNDALGEKAR, V. M. & GUPTA, A. S. 1977 On the dispersion of dye with a harmonically varying concentration in the hydromagnetic flow in a channel. *J. Appl. Phys.* **48**, 5344–5346.

SWANSON, C. A. 1978 A dichotomy of PDE Sturmian theory. *SIAM Rev.* **20**, 285–300.

TAYLOR, G. I. 1953 Dispersion of soluble matter in solvent flowing slowly through a tube. *Proc. R. Soc. Lond.* A **219**, 186–203.